Inorganic Chemistry

Article

Electron Exchange between α-Keggin Tungstoaluminates and a Well-Defined Cluster-Anion Probe for Studies in Electron Transfer

Yurii V. Geletii,[†] Craig L. Hill,[†] Alan J. Bailey,[†] Kenneth I. Hardcastle,[†] Rajai H. Atalla,[‡] and Ira A. Weinstock*,[§]

Department of Chemistry, Emory University, Atlanta, Georgia 30322, Chemistry and Pulping Research Work Unit, USDA Forest Products Laboratory, Madison, Wisconsin 50726, and Department of Chemistry, City College of The City University of New York, New York, New York 10031

Fully oxidized α-$Al^{III}W_{12}O_{40}^{5-}$ ($\mathbf{1}_{ox}$), and one-electron-reduced α-$Al^{III}W_{12}O_{40}^{6-}$ ($\mathbf{1}_{red}$), are well-behaved (stable and free of ion pairing) over a wide range of pH and ionic-strength values at room temperature in water. Having established this, ^{27}Al NMR spectroscopy is used to measure rates of electron exchange between $\mathbf{1}_{ox}$ (^{27}Al NMR: 72.2 ppm relative to $Al(H_2O)_6^{3+}$; $\nu_{1/2} = 0.77$ Hz) and $\mathbf{1}_{red}$ (74.1 ppm; $\nu_{1/2} = 0.76$ Hz). Bimolecular rate constants, k, are obtained from line broadening in ^{27}Al NMR signals as ionic strength, μ, is increased by addition of NaCl at the slow-exchange limit of the NMR time scale. The dependence of k on μ is plotted using the extended Debye–Hückel equation: $\log k = \log k_0 + 2\alpha z_1 z_2 \mu^{1/2}/(1 + \beta r \mu^{1/2})$, where z_1 and z_2 are the charges of $\mathbf{1}_{ox}$ and $\mathbf{1}_{red}$, α and β are constants, and r, the distance of closest contact, is fixed at 1.12 nm, the crystallographic diameter of a Keggin anion. Although not derived for highly charged ions, this equation gives a straight line ($R^2 = 0.996$), whose slope gives a charge product, $z_1 z_2$, of 29 ± 2, statistically identical to the theoretical value of 30. Extrapolation to $\mu = 0$ gives a rate constant k_{11} of $(6.5 \pm 1.5) \times 10^{-3}$ M^{-1} s^{-1}, more than 7 orders of magnitude smaller than the rate constant [$(1.1 \pm 0.2) \times 10^{5}$ M^{-1} s^{-1}] determined by ^{31}P NMR for self-exchange between $P^V W_{12}O_{40}^{3-}$ and its one-electron-reduced form, $P^V W_{12}O_{40}^{4-}$. Sutin's semiclassical model reveals that this dramatic difference arises from the large negative charges of $\mathbf{1}_{ox}$ and $\mathbf{1}_{red}$. These results, including independent verification of k_{11}, recommend $\mathbf{1}_{red}$ as a well-behaved electron donor for investigating outer-sphere electron transfer to molecules or nanostructures in water, while addressing a larger issue, the prediction of collision rates between uniformly charged nanospheres, for which $\mathbf{1}_{ox}$ and $\mathbf{1}_{red}$ provide a working model.

Introduction

This report addresses electron-transfer properties of polymeric metal–oxygen cluster anions (polyoxometalates or POMs).[1,2] These anions constitute a large and rapidly growing class of discrete molecular structures that includes small isopolyanions, such as $W_6O_{19}^{2-}$ (hexatungstate, less than 1 nm in diameter), slightly larger Keggin or Wells–Dawson heteropolyanions (e.g., $PMo_{12}O_{40}^{3-}$ or $P_2W_{18}O_{62}^{6-}$), and "giant wheel" oxomolydate nanoclusters[3,4] that contain 176 Mo cations (3.7 nm in diameter[5]). These and related polyoxoanions, and derivatives prepared by incorporation of main-group, transition-metal,[6,7] or f-block[8–11] cations, are used as molecular models for understanding magnetic

---

* Author to whom correspondence should be addressed. E-mail: iaw@sci.ccny.cuny.edu.

† Emory University.

‡ USDA Forest Products Laboratory.

§ City College of The City University of New York.

(1) Pope, M. T. In *Comprehensive Coordination Chemistry II: From Biology to Nanotechnology*; Wedd, A. G., Ed.; Elsevier Ltd.: Oxford, U. K., 2004; Vol. 4, pp 635−678.

(2) Hill, C. L. In *Comprehensive Coordination Chemistry II: From Biology to Nanotechnology*; Wedd, A. G., Ed.; Elsevier Ltd.: Oxford, U. K., 2004; Vol. 4, pp 679−759.

(3) Müller, A.; Roy, S. In *The Chemistry of Nanomaterials*; Rao, C. N. R., Müller, A., Cheetham, A. K., Eds.; Wiley-VCH: Weinheim, Germany, 2004; Vol. 1, pp 452−475.

(4) Yamase, T.; Prokop, P. V. *Angew. Chem., Int. Ed.* **2002**, *41*, 466−469.

(5) Müller, A.; Krickemeyer, E.; Bögge, H.; Schmidtmann, M.; Beugholt, C.; Kögerler, P.; Lu, C. *Angew. Chem., Int. Ed.* **1998**, *37*, 1220−1223.

(6) Lyon, D. K.; Miller, W. K.; Novet, T.; Domaille, P. J.; Evitt, E.; Johnson, D. C.; Finke, R. G. *J. Am. Chem. Soc.* **1991**, *113*, 7209−7221.

metallic oxides[12] and in applications that range from catalysis[13,14] and use as electron carriers in water-based fuel cells[12b] to the design of functional-nanocomposite materials.[15] As a class, POMs possess extensive and reversible redox chemistries.[16–18] In many applications, including catalysis,[19–22] functionality is vested in the electron-transfer properties[17,23–26] of these cluster anions.

We now use ^{27}Al NMR spectroscopy to obtain data that define electron exchange between a fully oxidized α-Keggin heteropolytungstate, α-$Al^{III}W_{12}O_{40}{}^{5-}$ ($\mathbf{1}_{ox}$),[27–30] and α-$Al^{III}W_{12}O_{40}{}^{6-}$ ($\mathbf{1}_{red}$), which contains a single d electron (Figure 1). A detailed understanding of electron self-exchange between Keggin structures[31] such as these is fundamental to the function of polytungstates in many of their diverse applications. Moreover, $\mathbf{1}_{ox}$, which is 1.12 nm in diameter,[27] may be viewed as a tetrahedral aluminate oxoanion, $Al^{III}O_4{}^{5-}$, encapsulated within a neutral, also tetrahedral, α-$W^{VI}_{12}O_{36}$ shell ("clathrate" model[29,32–34]). According to this model, the $Al^{III}O_4{}^{5-}$ oxoanion in $\mathbf{1}_{red}$ is located at the center of a
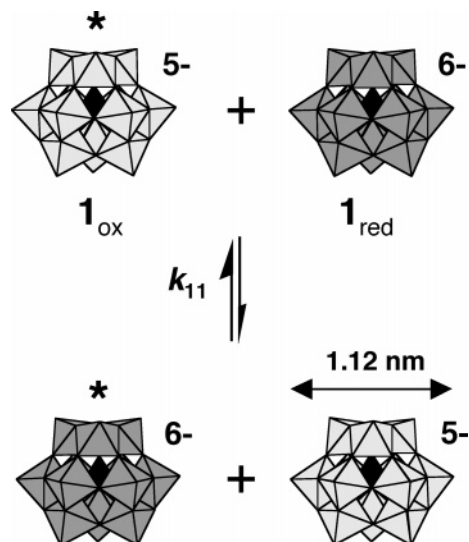
Figure 1. Electron exchange between α-$AlW_{12}O_{40}{}^{5-}$ ($\mathbf{1}_{ox}$) and α-$AlW_{12}O_{40}{}^{6-}$ ($\mathbf{1}_{red}$). The α-Keggin anions, shown in coordination-polyhedron notation, are 1.12 nm in diameter and possess tetrahedral (T_d) symmetry. In each anion, 12 W addendum atoms are at the center of WO_6 polyhedra, which each possess C_{4v} symmetry and have O atoms at their vertexes. At the center of each cluster (shaded) is a tetrahedral aluminate oxoanion, $Al^{III}O_4{}^{5-}$.

negatively charged $W_{12}O_{36}{}^{1-}$ shell,[35] which contains a single d (valence) electron. Self-exchange between $\mathbf{1}_{red}$ and $\mathbf{1}_{ox}$, thus, involves electron transfer into and out of $W_{12}O_{36}$ and $W_{12}O_{36}{}^{1-}$ structures. Insofar as the neutral, closest-packed $W_{12}O_{36}$ shell in $\mathbf{1}_{ox}$ represents the "solubilized" fragment[36] of an extended solid-state WO_3 lattice, electron exchange between $\mathbf{1}_{red}$ and $\mathbf{1}_{ox}$ also provides a molecular model for electron injection into early-transition-metal oxides.

In addition to a focus on electron exchange, we herein provide detailed aqueous solution-chemistry data needed to rigorously establish α-$AlW_{12}O_{40}{}^{6-}$ ($\mathbf{1}_{red}$) as a reliable mechanistic probe[37] for fundamental studies in electron transfer. These solution studies show that $\mathbf{1}_{red}$ is stable with respect to disproportionation, structural isomerization,[27,28] and hydrolysis[38] (from pH 0 to physiological pH values of larger than 7); remains unprotonated over a wide range of pH values (from pH 1.8 to 7.5); and is free of ion pairing[26,39,40] with Na^+ (present as POM countercations or as electrolyte), at Na^+ concentrations as large as 1 M. From combined electron-exchange and solution-chemistry studies, $\mathbf{1}_{red}$ emerges as a versatile, well-behaved, and kinetically well-defined outer-sphere probe[41] for investigating electron transfer to small molecules, biomimetic metallo-organic complexes (and possibly enzymes themselves), and for studying electron injection into nanoscale assemblies, such as low-poly-

(7) Anderson, T. M.; Neiwert, W. A.; Kirk, M. L.; Piccoll, P. M. B.; Schultz, A. J.; Koetzle, T. F.; Musaev, D. G.; Morokuma, K.; Cao, R.; Hill, C. L. *Science* **2004**, *306*, 2074–2077.
(8) Ozeki, T.; Yamase, T. *Acta Crystallogr., Sect. B* **1994**, *50*, 128–134.
(9) Luo, Q.; Howell, R. C.; Bartis, J.; Dankova, M.; Horrocks, W. D., Jr.; Rheingold, A. L.; Francesconi, L. C. *J. Inorg. Biochem.* **2002**, *41*, 6112–6117.
(10) Belai, N.; Dickman, M. H.; Pope, M. T.; Contant, R.; Keita, B.; Mbomekalle, I.-M.; Nadjo, L. *Inorg. Chem.* **2005**, *44*, 169–171.
(11) Zhang, C.; Howell, R. C.; Luo, Q.; Fieselmann, H. L.; Todaro, L. J.; Francesconi, L. C. *Inorg. Chem.* **2005**, *44*, in press.
(12) Clemente-Juan, J. M.; Coronado, E.; Gaita-Ariño, A.; Gimenez-Saiz, C.; Gudel, H.-U.; Sieber, S.; Bircher, R.; Mutka, H. *Inorg. Chem.* **2005**, *44*, 3389–3395.
(13) (a) Neumann, R. *Prog. Inorg. Chem.* **1998**, *47*, 317–370. (b) Kim, W. B.; Voitl, T.; Rodriguez-Riveera, G. J.; Dumesic, J. A. *Nature* **2004**, *305*, 1280–1283.
(14) Hill, C. L. *Chem. Rev.* **1998**, *98*, 1–389 (thematic issue on polyoxometalates).
(15) Yamase, T.; Pope, M. T. *Polyoxometalate Chemistry for Nanocomposite Design*; Kluwer Academic/Plenum Publishers: New York, 2002; Vol. 2.
(16) Pope, M. T. *Heteropoly and Isopoly Oxometalates*; Springer-Verlag: Berlin, 1983.
(17) Weinstock, I. A. *Chem. Rev.* **1998**, *98*, 113–170.
(18) Bi, L. H.; Kortz, U.; Nellutla, S.; Stowe, A. C.; van Tol, J.; Dalal, N. S.; Keita, B.; Nadjo, L. *Inorg. Chem.* **2005**, *44*, 896–903.
(19) Mizuno, N.; Nozaki, C.; Kiyoto, I.; Misono, M. *J. Am. Chem. Soc.* **1998**, *120*, 9267–9272.
(20) Weiner, H.; Finke, R. G. *J. Am. Chem. Soc.* **1999**, *121*, 9831–9842.
(21) Weinstock, I. A.; Barbuzzi, E. M. G.; Wemple, M. W.; Cowan, J. J.; Reiner, R. S.; Sonnen, D. M.; Heintz, R. A.; Bond, J. S.; Hill, C. L. *Nature* **2001**, *414*, 191–195.
(22) Bar-Nahum, I.; Khenkin, A. M.; Neumann, R. *J. Am. Chem. Soc.* **2004**, *126*, 10236–10237.
(23) Kozik, M.; Hammer, C. F.; Baker, L. C. W. *J. Am. Chem. Soc.* **1986**, *108*, 7627–7630.
(24) Toth, J. E.; Anson, F. C. *J. Am. Chem. Soc.* **1989**, *111*, 2444–2451.
(25) Kozik, M.; Baker, L. C. W. *J. Am. Chem. Soc.* **1990**, *112*, 7604–7611.
(26) Grigoriev, V. A.; Cheng, D.; Hill, C. L.; Weinstock, I. A. *J. Am. Chem. Soc.* **2001**, *123*, 5292–5307.
(27) Weinstock, I. A.; Cowan, J. J.; Barbuzzi, E. M. G.; Zeng, H.; Hill, C. L. *J. Am. Chem. Soc.* **1999**, *121*, 4608–4617.
(28) Cowan, J. J.; Bailey, A. J.; Heintz, R. A.; Do, B. T.; Hardcastle, K. I.; Hill, C. L.; Weinstock, I. A. *Inorg. Chem.* **2001**, *40*, 6666–6675.
(29) Neiwert, W. A.; Cowan, J. J.; Hardcastle, K. I.; Hill, C. L.; Weinstock, I. A. *Inorg. Chem.* **2002**, *41*, 6950–6952.
(30) Cowan, J. J.; Hill, C. L.; Reiner, R. S.; Weinstock, I. A. In *Inorg. Synth.*; Coucouvanis, D., Ed.; John Wiley & Sons: New York, 2002; Vol. 33, pp 18–26.
(31) Rasmussen, P. G.; Brubaker, J.; Carl, H. *Inorg. Chem.* **1964**, *3*, 977–980.
(32) Day, V. W.; Klemperer, W. G. *Science* **1985**, *228*, 533–541.
(33) Maestre, J. M.; Lopez, X.; Bo, C.; Poblet, J.-M.; Casañ-Pastor, N. *J. Am. Chem. Soc.* **2001**, *123*, 3749–3758.
(34) Lopez, X.; Maestre, J. M.; Bo, C.; Poblet, J.-M. *J. Am. Chem. Soc.* **2001**, *123*, 9571–9576.
(35) Lopez, X.; Poblet, J. M. *Inorg. Chem.* **2004**, *43*, 6863–6865.
(36) Fox, M. A.; Cardona, R.; Gaillard, E. *J. Am. Chem. Soc.* **1987**, *109*, 6347–6354.
(37) Eberson, L. *J. Am. Chem. Soc.* **1983**, *105*, 3192–3199.
(38) Kim, G.-S.; Zeng, H.; Neiwert, W. A.; Cowan, J. J.; VanDerveer, D.; Hill, C. L.; Weinstock, I. A. *Inorg. Chem.* **2003**, *42*, 5537–5544.
(39) Kirby, J. F.; Baker, L. C. W. *Inorg. Chem.* **1998**, *37*, 5537–5543.
(40) Kim, K. C.; Pope, M. T. *J. Am. Chem. Soc.* **1999**, *121*, 8512–8517.

dispersity colloidal suspensions of metal, metal-oxide, or semiconductor quantum dots.

To date, the most reliable measurements and accurate theoretical modeling of rate constants for electron self-exchange between heteropolyanions was reported by Kozik and Baker in 1990.[25] Using Sutin's semiempirical method,[42] they predicted the rate constant for self-exchange between $PW_{12}O_{40}^{4-}$ (2_{red}; one-electron reduced) and fully oxidized $PW_{12}O_{40}^{3-}$ (2_{ox}).[43] Close agreement was found between their predicted value (3.6×10^5 M^{-1} s^{-1}, at zero ionic strength) and the rate constant determined by analysis of line broadening in ^{31}P NMR spectra of aqueous mixtures of 2_{red} and 2_{ox} (1.1×10^5 M^{-1} s^{-1}). In the present study, the rate constant for self-exchange between 1_{red} and 1_{ox} is determined by analysis of line broadening in ^{27}Al NMR spectra[21,27,28] of mixtures of these Al(III)-centered cluster anions.

As reported below, the rate constant for electron exchange between oxidized and reduced forms of **1** is more than 7 orders of magnitude smaller than that reported for **2**. The theoretical basis for this, which resides in the very different ion charges, and the degrees of Coulombic repulsion that must be overcome in formation of contact ion pairs in the two exchanging systems ($[1_{red}:1_{ox}]^{11-}$ and $[2_{red}:2_{ox}]^{7-}$), is confirmed by a comparative analysis of both systems using Sutin's empirical model. To verify this, the rate constant for electron exchange between 1_{red} and 1_{ox} is confirmed by data from an entirely independent line of experimental evidence.

(41) Other electron-donating POMs have been used as mechanistic probes for investigating reductions of organic and inorganic molecules (cf., ref 17). One of these, $Co^{II}W_{12}O_{40}^{7-}$ (one W d electron), is similar to 1_{red} in that it appears to be stable to hydrolysis at near-neutral pH values. Our CV data indicate that $Co^{II}W_{12}O_{40}^{7-}$, because, unlike 1_{red}, it is a −7 ion, is protonated at pH values below 4 and, therefore, is not suitable for use in evaluating the effect of variation in pH ($[H^+]$) on electron-transfer reactions. (This is one of several criteria used to establish whether electron-transfer reactions that involve the making or breaking of C−H, O−H, or N−H and related bonds occur via simultaneous, proton-coupled electron transfer, or via sequential electron transfer followed by proton transfer). By contrast, 1_{red} remains unprotonated at pH values from 7 to less than 1.8. The relationship between Keggin-anion charge and pK_a warrants additional comment: For a series of isostructural protic bases, Brønsted basicities often increase with negative charge of the conjugate acid. This is true, as well, for isostructural α-Keggin anions, in which the monoprotic acids of the fully oxidized cluster anions, $H^+[X^{n+}W_{12}O_{40}]^{(n-8)-}$, become less acidic ($pK_a$ values increase) as cluster-anion charge increases. This occurs as heteroatom charge, n, becomes smaller (e.g., as X^{n+} varies from P^{5+} to Si^{4+} to Al^{3+} to Co^{2+}). The result is indicated by the pH dependence of reduction-potential, $E_{1/2}$, values (from CV data): For anion charges of −3 and −4 ($X^{n+} = P^{5+}$ and Si^{4+}), one-electron $E_{1/2}$ values are independent of pH from pH 7 to less than 1, for anion charges of −5 ($X^{n+} = Al^{3+}$), $E_{1/2}$ values are pH independent from pH 7 to less than 1.8, and for anion charges of −6 ($X^{n+} = Co^{2+}$), protonation of the one-electron-reduced (−7) anion, $[Co^{2+}W_{12}O_{40}]^{7-}$, is indicated by an increase in $E_{1/2}$ values (for the $[Co^{2+}W_{12}O_{40}]^{6-}$/$[Co^{2+}W_{12}O_{40}]^{7-}$ couple) as pH values reach 4 and below.
(42) Sutin, N. *Acc. Chem. Res.* **1982**, *15*, 275−282.
(43) While these anions are unprotonated at very low pH values (between 0 and 1), 2_{red} is not suitable for use as a mechanistic probe at most pH values. This is because 2_{ox} is unstable at pH values above ca. 1.8, and 2_{red} is susceptible to hydrolysis at only slightly higher pH values. By contrast, 1_{red} is stable to condensation or hydrolysis at pH values of 0 to greater than 7. Moreover, 1_{red} possesses a reduction potential more negative than that of 2_{red} by nearly 400 mV (i.e., it is a considerably stronger reducing agent). The pH stability and reduction potential of α-$SiW_{12}O_{40}^{5-}$ (one-electron reduced) lie between those of 2_{red} and 1_{red}.

Material and Methods

Synthesis and Characterization. The following, fully oxidized heteropolytungstates (all W atoms in their highest, +6 oxidation states and possessing d^0 electronic configurations), α- and β-Na_5-$Al^{III}W_{12}O_{40}$[27,28,30] and α-$K_5Co^{III}W_{12}O_{40}$,[44] were prepared using published methods; α-$Na_3P^VW_{12}O_{40} \cdot xH_2O$ was purchased from Sigma-Aldrich, Inc. One- and two-electron-reduced forms of α- and β-$Al^{III}W_{12}O_{40}^{5-}$, and of α-$P^VW_{12}O_{40}^{3-}$, were prepared in water by constant-potential electrolysis (see below) and stored under argon. All other materials were purchased from commercial sources.

Aqueous Solutions. To minimize concentrations of trace metals in kinetic studies, solutions were prepared using water from a Barnstead Nanopure water-purification system and the chemicals used (buffer, salts, and other additives) were of the highest purity available. Desired ionic strengths were obtained by additions of NaCl, and unless indicated otherwise, reported ionic-strength values include contributions from POM salts. pD values of solutions in D_2O were calculated using pD = pH_{el} + 0.4, where pH_{el} was read from a standard pH electrode immersed in the D_2O solution.[38,45] For 1:1 mixtures of D_2O and H_2O, pH values (calculated as pH_{el} + 0.2) are reported. Small deviations from target pH (pD) values, caused by additions of NaCl or POM salts to pH-adjusted buffered solutions, were compensated for by additions of very small quantities of appropriate acids or bases (typically HCl or NaOH).

Instrumentation. UV−vis spectra were acquired using Hewlett-Packard 8452A or StellarNet Inc. EPP2000 spectrophotometers equipped with diode-array detectors and immersible fiber-optic probes. The Hewlett-Packard 8452A instrument was equipped with a magnetic stirrer and temperature controller (HP 89090A). Electrochemical data were obtained at room temperature using a BAS CV-50W electrochemical analyzer equipped with a glassy-carbon working electrode, a Pt-wire auxiliary electrode, and a Ag/AgCl (3 M NaCl) BAS reference electrode. All reduction potentials are reported relative to the normal hydrogen electrode (NHE). pH measurements were made using an Orion 250A pH meter. In some experiments, reaction rates were measured using an SF-61 stopped-flow instrument (Hi-Tech Scientific, UK).

^{27}Al NMR Spectroscopy.[46] ^{27}Al NMR spectra were collected on a GE QE300 MHz spectrometer at 78.216 MHz, using a pulse width of 15 μs and a sweep width of 12 500 Hz. Reported chemical-shift values are referenced to 0.1 M $AlCl_3$ in 1.0 M aqueous HCl ($[Al(H_2O)_6]^{3+}$, $\delta = 0$ ppm) placed in the inner compartment of coaxial NMR tubes. The reference solutions were also used as external standards for integration of the ^{27}Al NMR signals. Internal lock signals were tuned using D_2O. Spectral data were processed using the NMR software package NUTS (1-D version, Acorn NMR Inc., Fremont, CA).

Electrochemistry. Cyclic Voltammetry and Reduction Potentials. Cyclic voltammograms (CVs) were obtained at room temperature using 1−6 mM POM concentrations in buffered solutions; ionic strengths of 0.05−1.20 M, adjusted by the addition of NaCl; a Ag/AgCl (3 M NaCl) BAS reference electrode; and scan rates of 20−400 mV s^{-1}. To obtain the highly accurate reduction potential ($E_{1/2}$) values needed for the assignment of $\Delta G°$ values to specific electron-transfer reactions, the BAS reference electrode was calibrated using the $[Fe(CN)_6]^{3-}$/$[Fe(CN)_6]^{4-}$ couple,

(44) For a convenient preparative method, see: Habib, M. H.; Tangestaninejad, S.; Mohammadpoor-Baltork, I.; Mirkhani, V.; Yadollahi, B. *Tetrahedron Lett.* **2001**, *42*, 2851−2853.
(45) Westcott, C. C. *Ph measurements*; Academic Press: New York, 1978.
(46) See ref 27 for more details concerning the acquisition and accurate integration of ^{27}Al NMR signals of heteropolyaluminates.

for which accurate published data are available.[47] On the basis of this calibration, $E_{1/2}$ values reported below, all of which were obtained using the BAS Ag/AgCl (3 M NaCl) reference electrode, are reported relative to the NHE by the addition of 250 mV to the BAS electrode values. (See the Supporting Information for details concerning the calibration and for control experiments that show that the 250 mV difference between the BAS electrode and NHE applies at the salt concentrations and ionic-strength values used in the present work.)

Bulk Electrolysis. Aqueous solutions of one- and two-electron-reduced α-Keggin anions were prepared by bulk electrolysis under Ar using a reticulated vitreous-carbon working electrode. The auxiliary electrode, a coiled Pt wire, was located in a separate compartment connected by fritted glass. The reactions were carried out using 0.1 M buffer solutions. Prior to electrolysis, ionic-strength values were adjusted by the addition of NaCl and desired pH values were reached by additions of small amounts of NaOH or HCl. For solutions used to determine electron self-exchange rate constants by NMR spectroscopy, 1:1 mixtures of D_2O and water were used. During electrolysis, vigorous agitation was provided by a magnetic stirrer and by agitation caused by the bubbling of Ar through the solution (air was rigorously excluded). The working electrode was typically set at a potential 120−180 mV more negative than that of the redox couple of the desired reduction (measured by CV in the same solution), and the number of Coulombs of charge passed was monitored continuously. In most cases, with POM concentrations of ca. 3 mM, total charges transferred, Q, were 3−7% (and sometimes 5−10%) higher than theoretical values ($Q = nFN$, where $n = 1$ or 2, F is the Faraday constant, and N is [POM]). pH (pD) values, measured before and after electrolysis reactions, typically varied by less than 0.1 unit. Samples for NMR spectroscopy were prepared by using a Hamilton gastight syringe to transfer 0.55 mL aliquots of catholite to Ar-filled NMR tubes already attached to a vacuum line. Once flame sealed, using standard Schlenk techniques, these tubes could be kept for several months without noticeable changes in NMR spectra.

Spectrophotometric Determination of Reduced α-Keggin Anion Concentrations. Extinction coefficients of reduced α-Keggin anions were determined by in situ UV−vis spectroscopic analysis of buffered POM solutions, carried out during bulk electrolysis. Prior to electrolysis, an immersible fiber-optic probe (connected to the EPP2000 spectrophotometer) was inserted into each solution of fully oxidized POM anion (POM$_{ox}$). Once electrolysis was begun, UV−vis spectra were recorded at regular intervals until successive spectra showed no further changes; the final spectrum was saved. This procedure was repeated using three or four different initial POM$_{ox}$ concentrations ([POM$_{ox}$]$_{initial}$). In each case, the final, saved spectra, in which [POM$_{red}$] = [POM$_{ox}$]$_{initial}$, were converted into plots of extinction coefficient, ϵ, versus wavelength (in nm). Irrespective of the [POM$_{ox}$]$_{initial}$ values used, these plots, which provided extinction coefficients over a wide range of wavelengths, varied from one another by less than 5%. Using this method, extinction coefficients at 700 nm for α-AlW$_{12}$O$_{40}$$^{6-}$ (1_{red}) were $1.7 \pm 0.1 \times 10^3$ and $1.9 \pm 0.1 \times 10^3$ M^{-1} cm^{-1}, respectively, in phosphate buffer at pH 7.2 and in sulfate buffer at pH 2.2. To verify that controlled-potential electrolysis gave the desired one- and two-electron-reduced POMs, and to provide an independent measurement of the extinction coefficient of 1_{red}, the following titrimetric method (described for the one-electron reduction of 1_{ox}) was used.

Titrimetric Determination of α-AlW$_{12}$O$_{40}$$^{6-}$ (1_{red}) Concentrations. Precise values for the extinction coefficient, ϵ, and concentrations in solution, of the one-electron-reduced anion, 1_{red}, were determined by titration[21] using α-K$_5$Co^{III}W$_{12}$O$_{40}$, a strong one-electron oxidant: $E_{1/2} = 1.05$ V (NHE) at pH values between 5.5 and 6.0.[48] For α-Co^{III}W$_{12}$O$_{40}$$^{5-}$, $\epsilon = 1090 \pm 30$ M^{-1} cm^{-1} at $\lambda_{max} = 390$ nm; for α-Co^{II}W$_{12}$O$_{40}$$^{6-}$, $\epsilon = 215 \pm 10$ M^{-1} cm^{-1} at $\lambda_{max} = 624$ nm. While 1_{red} absorbs strongly between 700 and 800 nm, α-AlW$_{12}$O$_{40}$$^{5-}$ (1_{ox}) has effectively no absorbance between 370 and 800 nm. Using this method (see the Supporting Information for details), an extinction coefficient for 1_{red} of $\epsilon_{700} = (1.85 \pm 0.10) \times 10^3$ M^{-1} cm^{-1} was obtained. This value is in good agreement with those determined by in situ UV−vis spectroscopy of dilute (<1 mM) 1_{red} solutions during and after bulk electrolysis [$(1.7 \pm 0.1) \times 10^3$ and $(1.9 \pm 0.1) \times 10^3$ M^{-1} cm^{-1}, respectively, at pH 7.2 and pH 2.2; see previous paragraph]. In subsequent kinetic studies, an average value of $\epsilon_{700} = (1.8 \pm 0.1) \times 10^3$ M^{-1} cm^{-1} was used. A plot of Q/unit volume versus [1_{red}] (the number of Coulombs of charge passed through the electrolysis cell per unit volume of electrolyte) gave a straight line with a slope of 95 300 $\pm$ 300 C mol^{-1}. Correspondence of this value to the Faraday constant ($F = 9.65 \times 10^3$ C mol^{-1}) confirmed that α-AlW$_{12}$O$_{40}$$^{5-}$ (1_{ox}) was reduced by one electron ($n = 1$ in $Q = nFN$, where N is the number of moles of 1_{red}).

X-ray Crystal Structure of α-Cs$_6$Na[AlW$_{12}$O$_{40}$]·14.5H$_2$O. Although 1_{red} is stable to disproportionation in *solution*,[49] efforts to grow X-ray quality crystals from solutions of 1_{red} invariably yielded crystals of the two-electron-reduced ion, α-AlW$_{12}$O$_{40}$$^{7-}$.[50] In typical syntheses, 0.3 g of α-Na$_5$AlW$_{12}$O$_{40}$ in 15 mL of water were reduced by bulk electrolysis at a series of potentials slightly more negative than that of the 1_{ox}/1_{red} couple. (The first one-electron reduction of 1_{ox} occurs at −130 mV versus NHE, and the potentials used in repeated attempts were slightly more negative than this value but, in all cases, substantially more positive than −330 mV, the potential at which 1_{red} is reduced by a second electron to give α-AlW$_{12}$O$_{40}$$^{7-}$). In all cases, solutions of 1_{red} obtained were free of α-AlW$_{12}$O$_{40}$$^{7-}$ (this was confirmed by ^{27}Al NMR spectroscopy). After electrolysis, 2 equivalents of Cs$^+$ were added to the dark blue solutions, and the volumes were reduced to 5 mL. After cooling overnight at 5 °C, low-yield mixtures of small blue crystals were obtained. Analysis of the small blue crystals by X-ray crystallography showed these to be a mixed (Cs$^+$ and Na$^+$) salt of α-AlW$_{12}$O$_{40}$$^{7-}$.

A suitable blue crystal of α-Cs$_6$Na[AlW$_{12}$O$_{40}$]·14.5H$_2$O was coated with Paratone N oil, suspended in a small fiber loop, and placed in a cooled nitrogen gas stream at 100 K on a Bruker D8 SMART APEX CCD sealed tube diffractometer with graphite monochromated Mo Kα (0.710 73 Å) radiation. Data were measured using a series of combinations of ϕ and Ω scans with 10 s frame exposures and 0.3° frame widths. Data collection, indexing, and initial cell refinements were all carried out using SMART[51] software. Frame integration and final cell refinements were done

(48) Carloni, P.; Eberson, L. *Acta Chem. Scand.* **1991**, *45*, 373−376.
(49) This is generally true for one-electron-reduced Keggin anions, and even for Cu^{I}W$_{12}$O$_{40}$$^{7-}$, obtained by one-electron reduction of Cu(II) in Cu^{II}W$_{12}$O$_{40}$$^{6-}$; see Pope, M. T.; Wexel, D. R. *J. Chem. Soc., Dalton Trans.* **1971**, *16*, 886−887 (reduction of Cu^{II}W$_{12}$O$_{40}$$^{6-}$) and Pope, M. T.; Varga, G. M., Jr. *Inorg. Chem.* **1996**, *5*, 1249−1254 (reductions of other Keggin anions).
(50) This result is consistent with the marked stabilities of reduced Keggin structures that contain even numbers of d electrons; see Fruchart, J. M.; Hervé, G.; Launay, J. P.; Massart, R. *J. Inorg. Nucl. Chem.* **1976**, *38*, 1627−1634.
(51) *Bruker AXS, I*, version 5.55; Analytical X-ray Systems: Madison, WI, 2000.

(47) Panzer, R. E.; Elving, P. J. *J. Electrochem. Soc.* **1972**, *119* (7), 864−874.

Table 1. Crystal Data for α-Cs$_6$Na[AlW$_{12}$O$_{40}$]·14.5H$_2$O

H$_{29}$AlCs$_6$NaO$_{54.5}$W$_{12}$	fw = 3954.86
a = 12.1412(12) Å	Z = 2
b = 13.1910(17) Å	$P\bar{1}$ (No. 2)
c = 18.5921(19) Å	T = −173(2) °C
α = 94.253(3)°	λ = 0.710 73 Å
β = 90.380(3)°	D_{calcd} = 4.719 g/cm^3
γ = 110.296(3)°	R1 ($I > 2\sigma(I)$)^a = 0.0612
V = 2783.4(5) Å^3	wR2 ($I > 2\sigma(I)$)^b = 0.1395

^{a} $R_1(F_o) = \sum ||F_o| - |F_c||/|F_o|$. ^{b} $wR(F_o{}^2) = [\sum w(F_o{}^2 - F_c{}^2)^2/\sum w F_o{}^4]^{1/2}$.

using SAINT[52] software. The final cell parameters were determined from least-squares refinement on 9999 reflections. The SADABS[53] program was used to carry out absorption corrections. The structure was solved using direct methods and difference Fourier techniques (SHELXTL, version 5.10).[54] All non-hydrogen atoms were refined anisotropically except for O35, O38, O3W, O15W, and O16W. Scattering factors and anomalous dispersion corrections were taken from the International Tables for X-ray Crystallography.[55] There was a small degree of disorder within the crystal, which is frequently the case for highly symmetrical Keggin anions. Considerable effort was made to model this disorder and to critically evaluate the number of Cs$^+$ and Na$^+$ cations, and water molecules, in the unit cell (see the Supporting Information for details). The structure solution, refinement, graphics, and generation of publication materials were performed using SHELXTL version 5.10 software. Additional details are given in Table 1 and in the Supporting Information.

Reaction-Rate Measurements. Electron self-exchange rate constants for reactions between α-AlW$_{12}$O$_{40}$$^{6-}$ (**1**$_{red}$) and α-AlW$_{12}$O$_{40}$$^{5-}$ (**1**$_{ox}$) were obtained by an analysis of line broadening in ^{27}Al NMR spectra of mixtures of **1**$_{red}$ and **1**$_{ox}$ as a function of ionic strength, and at several pH values (see Results and Discussion sections). Independent support for the zero ionic strength ($\mu = 0$ M) self-exchange rate constant, k_{11}, obtained by ^{27}Al NMR, was provided by using a stopped-flow apparatus (and UV−vis spectrometer) to determine the rate constant at zero ionic strength for the cross-reaction: **1**$_{red}$ + α-PW$_{12}$O$_{40}$$^{4-}$ (one-electron reduced, **2**$_{red}$) → **1**$_{ox}$ + α-PW$_{12}$O$_{40}$$^{5-}$ (two-electron reduced).

Bulk electrolysis was used to reduce solutions of 3.0 mM **1**$_{ox}$ and (separately) of 5.0 mM α-PW$_{12}$O$_{40}$$^{3-}$, in 50 mM sodium phosphate buffer (pH = 2.15, μ = 26 mM), at three [NaCl] values, 25, 50, and 100 mM NaCl. POM$_{red}$ solutions were then diluted quantitatively: [**1**$_{red}$] was between 0.06 mM and 0.08 mM, and [**2**$_{red}$] (molar excess) ranged from 0.5 to 2 mM. Desired ionic-strength values were obtained by adding NaCl to the 50 mM sodium phosphate buffer solutions. Concentrations of individual solutions of **1**$_{red}$ and **2**$_{red}$ were quantified by UV−vis spectroscopy at 700 nm, at which the extinction coefficients, ϵ, for both anions are at a maximum (1.8 × 10^3 M^{-1} cm^{-1} for **1**$_{red}$ and 1.66 × 10^3 M^{-1} cm^{-1} for **2**$_{red}$; see Figure S2 in the Supporting Information). All stopped-flow experiments were carried out under Ar, with [**2**$_{red}$]$_o$ always much larger than [**1**$_{red}$]$_o$, and for each reaction, kinetic data was extracted from the entire absorbance-versus-time curve. Reaction rates were determined by measuring the increase with time of absorbance at 480 nm, where the difference between the extinction

Table 2. First and Second One-Electron Reduction Potentials of α-XW$_{12}$O$_{40}$$^{n-}$, Relative to the Normal Hydrogen Electrode (NHE)

X	$-n/-(n+1)$	pH range	E, mV	E, mV (from ref 6)^a
Al	−5/−6	1.8−7.5	−130	
Al	−6/−7	2.05	−330	
Al	−6/−7	3.00	−350	
Al	−6/−7	7.2	−360	
Si	−4/−5	1.0−4.5	55	54
Si	−5/−6	1.0−4.5	−205	−204
P	−3/−4	1.0−2.0	255	218
P	−4/−5	1.0	−15	25

^{a} The numbers reported in ref 6 were obtained by polarography in 1 M sodium sulfate buffer; our data were obtained by CV and in conditions more typical of our kinetic studies: 0.05 M buffer solutions and 0.15 M NaCl.

coefficients of two-electron- and one-electron-reduced POM ions is largest (extinction coefficients at 480 nm are 3.1 × 10^3, 0.92 × 10^3, and 0.84 × 10^3 M^{-1} cm^{-1}, respectively, for α-PW$_{12}$O$_{40}$$^{5-}$, α-AlW$_{12}O_{40}$$^{6-}$, and α-PW$_{12}O_{40}$$^{4-}$; Figure S2, Supporting Information). The increase in absorbance was exponential, and an apparent monomolecular (pseudo-first-order) rate constant was determined from the kinetic traces (conversions were typically greater than 90%) using standard kinetics software (KISS 5.1 for Macintosh). Plots of observed rate constants as a function of [α-PW$_{12}$O$_{40}$$^{4-}$]$_o$ gave straight lines whose slopes were used to calculate bimolecular rate constants for the cross-reaction at each ionic strength studied.

Results

Formation, Redox Properties, and Stability of α-AlW$_{12}$O$_{40}$$^{6-}$ (1$_{red}$). Formation. Solutions of the one-electron-reduced anion, α-AlW$_{12}$O$_{40}$$^{6-}$ (**1**$_{red}$), were prepared by controlled-potential electrolysis. Quantitative formation of **1**$_{red}$ [$\epsilon_{700} = (1.8 \pm 0.1) \times 10^3$ M^{-1} cm^{-1}] was confirmed, as described above (see the Materials and Methods section), by UV−vis spectroscopy of the electrolyzed solutions and (even more accurately) after redox titration using Co^{III}W$_{12}$O$_{40}$$^{5-}$ as an oxidant.[17,21]

Reduction Potentials. The reduction potentials of the α-AlW$_{12}$O$_{40}$$^{5-}$/α-AlW$_{12}O_{40}$$^{6-}$ (**1**$_{ox}$/**1**$_{red}$) and α-PW$_{12}$O$_{40}$$^{3-}$/α-PW$_{12}O_{40}$$^{4-}$ (**2**$_{ox}$/**2**$_{red}$) couples, and others, were measured in pH-buffered NaCl-electrolyte solutions by cyclic voltammetry (a representative CV is included in the Supporting Information). Results for a series of couples, at pH values dictated by ion stabilities, are provided in Table 2 (α-SiW$_{12}$O$_{40}$$^{4-}$ and published values[56] obtained under similar, but not identical, conditions are included for comparison).

pH Independence of the 1$_{ox}$/1$_{red}$ Couple. The oxidized and reduced forms of **1** uniquely possess two complementary characteristics critical to the use of **1**$_{red}$ in variable-pH kinetic studies: (1) both **1**$_{ox}$ and **1**$_{red}$ are stable in water at room temperature over pH values of 0−7.5,[27,28] and (2) the reduction potential of the **1**$_{ox}$/**1**$_{red}$ couple remains constant as pH values are decreased from 7.5 to 1.8. This invariance in the reduction potential shows that, even at acidic pH values, **1**$_{red}$, a −6 anion, remains unprotonated; that is, no observable ion pairing with H$^+$ (or with Na$^+$, present as an electrolyte) occurs.[26] This absence of protonation, and of ion pairing generally, eliminates a complicating factor that is

(52) *BrukerAXS, I.*, version 6.02; Analytical X-ray Systems: Madison, WI, 1999.
(53) Sheldrick, G. *SADABS*; University of Göttingen: Göttingen, Germany, 1996.
(54) *Bruker AXS, I.*, version 5.10; Analytical X-ray Systems: Madison, WI, 1997.
(55) *Internation Tables for X-ray Crystallography*; Kynoch Academic Publishers: Dordrecht, The Netherlands, 1992; Vol. C.

(56) Pope, M. T.; Varga, G. M., Jr. *Inorg. Chem.* **1966**, *5*, 1249−1254.

typically difficult to avoid in studies of outer-sphere electron-transfer processes involving charged reactants.[17,57−59]

Stability in Aqueous Solution. Solution studies were carried out to establish that, at room temperature in pH-buffered aqueous solutions, pure 1_{red} is stable with respect to three plausible processes: (1) isomerization to the β-Keggin structure;[27,28,34] (2) disproportionation to mixtures of 1_{ox}, 1_{red}, and the two-electron-reduced anion α-AlW$_{12}$O$_{40}$$^{7-}$; and (3) acid decomposition at low pH values, or hydrolysis at neutral pH values, to give defect "lacunary" species with less than a full complement of 12 W "addendum" atoms.[27,28,30] These points are addressed in the following control experiments.

First, ^{27}Al NMR spectra of ca. 5 mM solutions of pure α-AlW$_{12}$O$_{40}$$^{5-}$ (1_{ox}) at pH 7.2 (50 mM phosphate buffer) are unchanged after 24 h. Moreover, equilibrated solutions of mixtures of 1_{ox} and 1_{red}, and of mixtures of 1_{red} and the two-electron-reduced anion α-AlW$_{12}$O$_{40}$$^{7-}$, prepared by bulk electrolysis as described above, were stored at room temperature in flame-sealed NMR tubes. After 6 months, no changes were observed by ^{27}Al NMR spectroscopy.[60] No β isomers or decomposition products were observed. In addition, ratios of oxidized-to-reduced anions remained unchanged, indicating that disproportionation of 1_{red} to give α-AlW$_{12}$O$_{40}$$^{7-}$ and 1_{ox} did not occur.

Disproportionation of 1_{red} to give 0.5 equivalents each of α-AlW$_{12}$O$_{40}$$^{7-}$ and 1_{ox} was unequivocally ruled out by deliberately mixing α-AlW$_{12}$O$_{40}$$^{7-}$ with an excess of 1_{ox} at pH 7.2 in a phosphate buffer. The reaction, followed by UV−vis spectroscopy, proceeded to completion. The absorbance of the solution was followed at 480 nm, where the difference between the extinction coefficients of the one-electron- and two-electron-reduced anions—1_{red} and α-AlW$_{12}$O$_{40}$$^{7-}$—is at its largest, 0.92×10^3 versus 2.3×10^3 M^{-1} cm^{-1}, respectively.

Previous observations[27,28] suggested that Keggin undecatungstoaluminates (α and β isomers of α-AlW$_{12}$O$_{40}$$^{5-}$, α-AlW$_{12}O_{40}$$^{6-}$, and α-AlW$_{12}O_{40}$$^{7-}$) are stable to hydrolysis at room temperature over a wide range of pH values (from less than 0 to larger than 7). This was confirmed quantitatively by cyclic voltammetry and ^{27}Al NMR spectroscopy. First, CVs (peak currents, peak separations, and reduction potentials) remained unchanged throughout repeated cycles of electrochemical reduction/reoxidation and before and after bulk electrolytic reduction at pH 7.2, in phosphate buffer (see Table S1 in the Supporting Information). CVs also remained unchanged when electrochemically reduced solutions of **1** were reoxidized by exposure to dioxygen (O$_2$ in
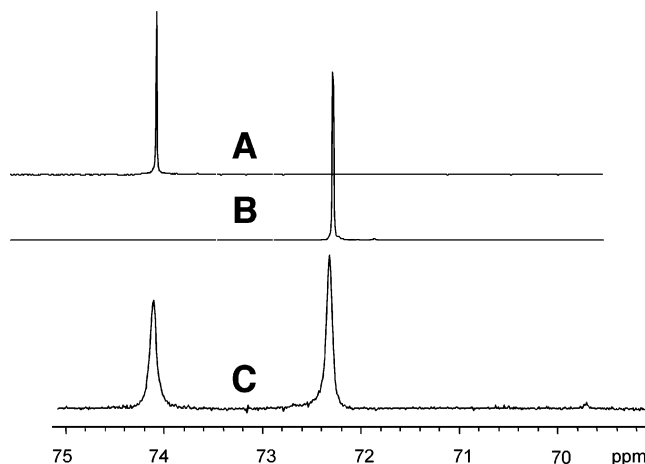
(57) Marcus, R. A. *J. Phys. Chem. B* **1998**, *102*, 10071−10077.
(58) Chen, P.; Meyer, T. J. *Chem. Rev.* **1998**, *98*, 1439−1477.
(59) Zahl, A.; van Eldik, R.; Swaddle, T. W. *Inorg. Chem.* **2002**, *41*, 757−764.
(60) Relative to the β isomer, the α isomer of 1_{ox} appears to be the major species present, i.e., highly favored thermodynamically, at pH 7 at room temperature. Also, while at very low pH values and high temperatures (e.g., 0.5 M H$^+$ and 200 °C) the β isomer is present at appreciable concentrations (ca. 15% at equilibrium, which is only attained after several days at 200 °C), at pH 1, isomerization of α to β is slow at temperatures between 0 and 80 °C. (The temperature dependence of the equilibrium constant for isomerization in 0.5 M H$^+$ is unknown.) For more details, see refs 27 and 28.

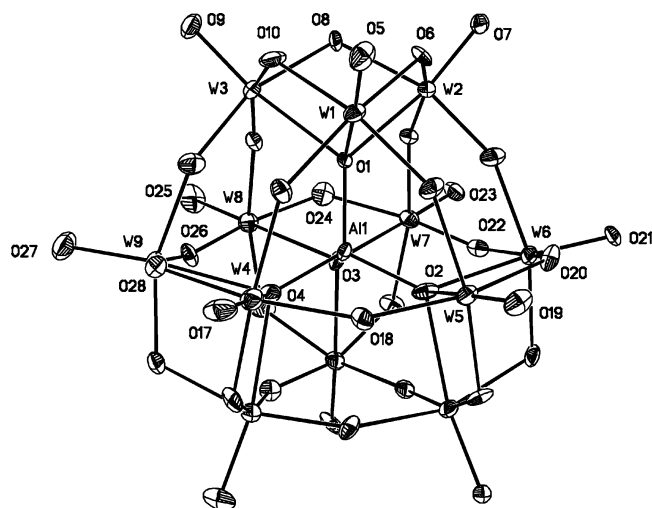**Figure 2.** ^{27}Al NMR spectra of α-AlW$_{12}$O$_{40}$$^{6-}$ (1_{red}, **A**), α-AlW$_{12}$O$_{40}$$^{5-}$ (1_{ox}, **B**), and a mixture containing a 1.0:0.85 molar ratio of 1_{ox} to 1_{red} (**C**). The total concentration of POM anions present ([1_{ox}] + [1_{red}]) was 4.6 mM; [NaCl] was 0.68 M at pH 7.2 and 19.2 ± 0.5 °C.

ambient air); no differences were observed between these solutions and those subjected to electrochemical reduction/reoxidation cycles. So, too, the ^{27}Al NMR spectra of all these solutions (number, location, intensities, and line widths of the ^{27}Al NMR signals) also remained unchanged (Table S1, Supporting Information). Therefore, the reduction and chemical- or electrochemical-oxidation processes are all reversible, neither altering POM concentrations nor resulting in detectable quantities of isomerization, disproportionation, or hydrolysis products.

Electron Self-Exchange between 1_{red} and 1_{ox}. Line Broadening in ^{27}Al NMR Spectra of Equilibrated Solutions. The rate constant for electron self-exchange between 1_{red} and 1_{ox} at zero ionic strength, $\mu = 0$, was determined by an analysis of line broadening in ^{27}Al NMR signals (Figure 2) as a function of ionic strength in 1:1 D$_2$O/H$_2$O mixtures.

Before relying upon ^{27}Al NMR spectra as a source of accurate self-exchange rate data, it was necessary to demonstrate that the broadening observed in mixtures of 1_{ox} and 1_{red} was due exclusively to electron exchange, and not to effects attributable to the nature of the quadrupolar ($I = ^5/_2$) ^{27}Al nucleus or to the fact that 1_{red} (one unpaired electron) is a paramagnet. Because ^{27}Al possesses a nuclear spin of $^5/_2$, narrow ^{27}Al NMR signals are only observed when the Al atom resides in a site of high symmetry. The overall T_d symmetry of 1_{ox} reflects the nearly ideal T_d geometry about the four-coordinate Al(III) ion at its center.[27] As a result of this high overall (cluster) and local (Al^{III}O$_4$$^{5-}$ oxoanion) symmetry, the ^{27}Al NMR spectrum of 1_{ox} contains a single, narrow signal ($\nu_{1/2} = 0.77 \pm 0.05$ Hz; Figure 2B).[27]

The ^{27}Al NMR signal due to the Al(III) heteroatom in 1_{red} is also very narrow ($\nu_{1/2} = 0.76 \pm 0.05$ Hz; Figure 2A). This demonstrates that one-electron reduction has not decreased the symmetry about the central heteroatom. Efforts to provide support for this conclusion by X-ray crystallography were inconclusive. First, attempts to obtain X-ray quality crystals of 1_{red} were unsuccessful. Solutions of 1_{red} invariably gave crystals of 1_{ox} and the two-electron-reduced ion, α-AlW$_{12}$O$_{40}$$^{7-}$, but not of 1_{red}.[50] Nonetheless, the two-

Figure 3. Thermal ellipsoid plot of α-AlW$_{12}$O$_{40}$$^{7-}$ (ellipsoids shown at 50% probability).

Table 3. Selected Bond Lengths (Å) and Angles (deg) of α-AlW$_{12}$O$_{40}$^{7}

bond	length (Å)	angle	degrees
Al(1)−O(1)	1.753(10)	O(1)−Al(1)−O(2)	109.7(5)
Al(1)−O(2)	1.753(13)	O(1)−Al(1)−O(3)	109.2(6)
Al(1)−O(3)	1.756(13)	O(1)−Al(1)−O(4)	108.8(6)
Al(1)−O(4)	1.753(14)	O(2)−Al(1)−O(3)	108.5(6)
O(1)−W(1)	2.245(10)	O(3)−Al(1)−O(4)	110.2(6)
O(1)−W(2)	2.250(11)	O(2)−Al(1)−O(4)	110.3(6)
O(1)−W(3)	2.266(11)	Al(1)−O(1)−W(1)	122.4(6)
W(1)−O(6)	1.958(11)	Al(1)−O(1)−W(2)	121.0(6)
W(2)−O(6)	1.940(11)	Al(1)−O(1)−W(3)	121.7(5)
W(1)−O(5)	1.715(11)	Al(1)−O(2)−W(5)	121.3(6)
W(2)−O(13)	1.845(11)	W(3)−O(16)−W(9)	152.7(7)
W(6)−O(13)	2.010(11)	W(2)−O(13)−W(6)	148.7(6)

electron-reduced anion, α-AlW$_{12}$O$_{40}$$^{7-}$, was structurally characterized (Table 3 and Figure 3). The line width of Al-(III) in α-AlW$_{12}$O$_{40}$$^{7-}$ is $\nu_{1/2} = 1.5 \pm 0.1$ Hz, slightly larger than that of Al(III) in $\mathbf{1}_{ox}$ or $\mathbf{1}_{red}$. In α-AlW$_{12}$O$_{40}$$^{7-}$, as in $\mathbf{1}_{ox}$ (previously structurally characterized[27]), the central Al(III) atom is at the center of a nearly ideal tetrahedron of four oxygen atoms [in both $\mathbf{1}_{ox}$ and α-AlW$_{12}$O$_{40}$$^{7-}$, bond lengths and angles about Al(III) show only slight, and similar, departures from perfect tetrahedral symmetry]. Notably, however, some intertriad W−μ-O−W bond lengths in α-AlW$_{12}$O$_{40}$$^{7-}$ are longer than analogous bond lengths in $\mathbf{1}_{ox}$. In α-AlW$_{12}$O$_{40}$$^{7-}$, for example, W(2)−O(13) and O(13)−W(6) are 1.845(11) and 2.010(11) Å, respectively, while other structurally analogous bonds in α-AlW$_{12}$O$_{40}$$^{7-}$ are close to 1.9 Å. This distortion, if not simply the result of packing forces or of association of the anion with countercations in the solid state, could explain why the line width observed for α-AlW$_{12}$O$_{40}$$^{7-}$ is slightly larger than that observed for $\mathbf{1}_{red}$. However, because the precise nature of d electrons in Keggin structures has yet to be fully clarified,[61−63] it is difficult to assess whether the reduction of $\mathbf{1}_{red}$ by a second electron would be expected to induce structural distortion.

At the same time, support for possible distortion in α-AlW$_{12}$O$_{40}$$^{7-}$ in solution is provided by structural and spectroscopic comparisons with β-AlW$_{12}$O$_{40}$$^{5-}$ (the β isomer of $\mathbf{1}_{ox}$). Although crystallographic data[29] show the central Al^{III}O$_4$$^{5-}$ fragment in β-AlW$_{12}$O$_{40}$$^{5-}$ to be a nearly ideal tetrahedron, the symmetry of the W$_{12}$O$_{36}$ shell has decreased

Table 4. Chemical Shifts (ppm) and Line widths (Hz) of Al(III)-Heteroatom Signals in ^{27}Al NMR Spectra of Fully Oxidized and One- and Two-Electron-Reduced α- and β-Dodecatungstoaluminates

entry	anion	chemical shift,[a] ppm	line width, Hz
1	α-AlW$_{12}$O$_{40}$$^{5-}$ ($\mathbf{1}_{ox}$)	72.3	0.77 ± 0.05
2	α-AlW$_{12}$O$_{40}$$^{6-}$ ($\mathbf{1}_{red}$)	74.1	0.76 ± 0.05
3	α-AlW$_{12}$O$_{40}$$^{7-}$ (2e$^-$ reduced)	68.9	1.5 ± 0.1
4	β-AlW$_{12}$O$_{40}$$^{5-}$ (β-$\mathbf{1}_{ox}$)	71.9	3.9 ± 0.2
5	β-AlW$_{12}$O$_{40}$$^{6-}$ (β-$\mathbf{1}_{red}$)	69.7	4.25 ± 0.2
6	β-AlW$_{12}$O$_{40}$$^{7-}$ (2e$^-$ reduced)	68.3	25 ± 8

[a] Relative to AlCl$_4$$^-$ (at pH = 1 in H$_2$O). Conditions: 19.2 ± 0.5 °C, pH/pD = 7.2 (H$_2$O/D$_2$O = 1:1).

from T_d (for α) to C_{3v} (for β). This results in a 5-fold increase in line width of the ^{27}Al NMR signal of 0.77 ± 0.05 Hz for α-AlW$_{12}$O$_{40}$$^{5-}$ ($\mathbf{1}_{ox}$) to 3.9 Hz for β-AlW$_{12}$O$_{40}$$^{5-}$. Hence, slight distortion in the W$_{12}$O$_{36}$ shell of α-AlW$_{12}$O$_{40}$$^{7-}$ could result in the broadening of its ^{27}Al NMR signal relative to that of $\mathbf{1}_{red}$. By contrast, the line widths of the ^{27}Al NMR signals in $\mathbf{1}_{red}$ and $\mathbf{1}_{ox}$ are statistically identical. This shows that little if any structural distortion occurs upon the reduction of $\mathbf{1}_{ox}$ to $\mathbf{1}_{red}$.

The line broadening in Figure 2 is also not due to the effect of unpaired electron spin on the ^{27}Al nucleus. While the precise location(s) and nature of electrons in reduced Keggin anions have yet to be fully clarified, it is known that the presence of a single, unpaired electron has no observable effect on the line widths of NMR signals of heteroatoms in other α-Keggin anions.[25,63] For example, narrow signals are observed in the ^{31}P NMR spectra [P(V), $I = ^1/_2$] of fully oxidized α-PW$_{12}$O$_{40}$$^{3-}$ and of the one- and two-electron-reduced forms of this anion.[23,25] Similarly, no paramagnetic broadening is observed in the ^{27}Al NMR spectra of $\mathbf{1}_{red}$.

The above conclusions hold true for α anions. As shown in Table 4, however, ^{27}Al line widths in the ^{27}Al NMR spectra of β isomers increase from 3.9 to 4.25 Hz for the fully oxidized and one-electron-reduced anions (β-AlW$_{12}$O$_{40}$$^{5-}$ and β-AlW$_{12}$O$_{40}$$^{6-}$, respectively) to 25 ± 5 Hz for the two-electron-reduced β anion. While beyond the scope of the present work, these data suggest that sensitivity of the quadrupolar ($I = ^5/_2$) ^{27}Al nucleus to subtle changes in anion symmetry might provide insight into the electronic structure of two-electron-reduced Keggin anions.

Self-Exchange Rate Constant. Rates of electron exchange as a function of ionic strength, μ (varied by addition of NaCl), were measured by a line-width analysis of ^{27}Al NMR spectra of equilibrated mixtures of fully oxidized and one-electron-reduced α-AlW$_{12}$O$_{40}$$^{6-}$ ($\mathbf{1}_{red}$) and α-AlW$_{12}$O$_{40}$$^{5-}$ ($\mathbf{1}_{ox}$) (Figure 2). While slight broadening of the ^{27}Al NMR signals occurred upon mixing, no changes in the chemical shifts of these

(61) DFT calculations (ref 35), which, for two-electron-reduced α-Keggin ions, place both electrons in a single LUMO constructed by the linear combination of d$_{xy}$ orbitals from all 12 W atoms, provide an experimentally accurate model for evaluating Keggin-anion reduction potentials. At the same time, spectroscopic data suggest that d electrons in reduced Keggin anions are rapidly exchanged between the 12 W ions (see refs 50, 62, and 63).

(62) Varga, G. M., Jr.; Papaconstantinou, E.; Pope, M. T. *Inorg. Chem.* **1970**, *9*, 662−667.

(63) Kazansky, L. P.; McGarvey, B. R. *Coord. Chem. Rev.* **1999**, *188*, 157−210.

Table 5. Bimolecular Rate Constants at Constant Ionic Strength[a]

entry	α-AlW$_{12}$O$_{40}$$^{5-}$ (1$_{ox}$), mM	α-AlW$_{12}$O$_{40}$$^{6-}$ (1$_{red}$), mM	Δν$_{ox}$, Hz	Δν$_{red}$, Hz	k[b] (×10^{-3}), M^{-1} s^{-1}	k[c] (×10^{-3}), M^{-1} s^{-1}
1	4.6	0	0.77 ± 0.05			
2	0	4.6		0.76 ± 0.05		
3	1.05	3.55	1.88	0.94	1	
4	2.85	1.75	1.38	1.47	1.05	0.85
5	3.95	0.65	1.01	1.9	1.15	0.92
					average:	1.0 ± 0.15

[a] pH = 7.2 (measured in 1:1 H$_2$O/D$_2$O), 50 mM NaH$_2$PO$_4$/Na$_2$HPO$_4$ buffer (i.e., 50 mM PO$_4$$^{3-}$), 0.1 M NaCl, total ionic strength, μ = 0.275 ± 0.02 M, 19.2 ± 0.5 °C. [b] Calculated using eq 3. [c] Calculated using eq 4.

signals were observed. This indicates that electron exchange is slow relative to the time scale of the NMR experiment.[23,25,64] At this slow-exchange limit, the line widths increase with an increase in either the concentration of the reactants (POM ions) or ionic-strength values. Kozik and Baker quantified rates of bimolecular electron exchange between POM ions in water by the analysis of changes in ^{31}P NMR signals as a function of ionic strength.[23,25] In mixtures of α-PW$_{12}$O$_{40}$$^{4-}$ (one-electron reduced, 2$_{red}$) and α-PW$_{12}$O$_{40}$$^{3-}$ (fully oxidized, 2$_{ox}$), and mixtures of α-PW$_{12}$O$_{40}$$^{5-}$ (two-electron reduced) and 2$_{red}$, ^{31}P NMR signals coalesced as ionic-strength values increased (rapid-exchange limit). On the other hand, electron transfer between fully oxidized and one-electron-reduced Wells−Dawson anions (α-P$_2$W$_{18}$O$_{62}$$^{6-}$ and α-P$_2$W$_{18}$O$_{62}$$^{7-}$) occurred at the slow-exchange limit. In the present case, involving a slow exchange between 1$_{red}$ and 1$_{ox}$, a quantitative analysis of ^{27}Al NMR line-width data was carried out using the method applied by Kozik and Baker to ^{31}P NMR spectra of the Wells−Dawson anions.

As in self-exchange between 2$_{red}$ and 2$_{ox}$,[23,25] and in related examples,[17] the reaction obeys the following rate expression:

$$\text{rate} = k[\mathbf{1}_{\text{red}}][\mathbf{1}_{\text{ox}}] \tag{1}$$

where k is the bimolecular rate constant for the reaction between 1$_{red}$ and 1$_{ox}$. The line width, Δν$_{red}$, of the ^{27}Al NMR signal of 1$_{red}$, at equilibrium in solution with 1$_{ox}$, is given by

$$\Delta\nu_{\text{red}} = 1/(\pi T_{\text{mixture}}) = 1/(\pi T_2) + 1/(\pi\tau) \tag{2}$$

where T_{mixture} is the total relaxation time associated with 1$_{red}$ at equilibrium in solution with 1$_{ox}$, T_2 is the relaxation time of pure 1$_{red}$, τ is the lifetime of 1$_{red}$ in its reaction with 1$_{ox}$, $1/(\pi T_2)$ is the line width of pure 1$_{red}$ (Δν$_{red}$^{0}), and $\tau = 1/(k[\mathbf{1}_{\text{ox}}])$. Substitution and rearrangement give

$$k = (\Delta\nu_{\text{red}} - \Delta\nu_{\text{red}}{}^0)\pi/[\mathbf{1}_{\text{ox}}] \tag{3}$$

Equation 3 gives the rate constant for self-exchange, k, as a function of line broadening in the ^{27}Al NMR signal of 1$_{red}$. Similarly, k, as a function of broadening in the ^{27}Al NMR signal of 1$_{ox}$, at equilibrium with 1$_{red}$, is given by

$$k = (\Delta\nu_{\text{ox}} - \Delta\nu_{\text{ox}}{}^0)\pi/[\mathbf{1}_{\text{red}}] \tag{4}$$

where Δν$_{ox}$^{0} is the line width of pure 1$_{ox}$.

Table 6. Bimolecular Rate Constants[a] at Several Ionic Strength Values[b]

entry	ionic strength, μ, M	k[b] (×10^{-3}), M^{-1} s^{-1}
1	0.18	0.35
2	0.23	0.54
3	0.265	0.95
4	0.275	1.0
5	0.43	2.15
6[c]	0.45	1.9[c]
7[c]	0.56	3.1[c]
8	0.58	4.1
9[d]	0.58	5.2[d]
10	0.73	6.4
11	0.867	7.1
12	1.1	11

[a] Each rate constant is an average of at least four ^{27}Al NMR measurements. [b] Unless indicated, [POM$_{total}$] = 4.6 mM, and reactions were carried out at 19.2 ± 0.5 °C in phosphate buffer (pH = 7.2), adjusted to 50 mM in 1:1 D$_2$O/H$_2$O. [c] [POM$_{total}$] = 9.2 mM. [d] pH = 2.15.

Rate constants were calculated from changes in the line widths of ^{27}Al NMR signals of each ion, 1$_{ox}$ and 1$_{red}$, present in solution at three different concentration ratios (Table 5). At constant ionic strength (μ), and constant [POM$_{total}$] (POM$_{total}$ = sum of concentrations of 1$_{ox}$ and 1$_{red}$), k is independent of the *relative* concentrations of 1$_{ox}$ and 1$_{red}$. This confirms the first-order dependence of k on [1$_{red}$], and on [1$_{ox}$], in eq 1.

Rate constants, k (rate = $k[\mathbf{1}_{\text{ox}}][\mathbf{1}_{\text{red}}]$), were then obtained from measurements of ^{27}Al NMR spectra as the ionic strength, μ, was varied (addition of NaCl) at the slow-exchange limit. Rate constants, k, at specific ionic-strength values, and at two pH values, are listed in Table 6. The functional dependence of log k on μ was calculated using the extended Debye−Hückel equation:[65] log k = log k_0 + $2\alpha z_1 z_2\mu^{1/2}/(1 + \beta r\mu^{1/2})$ (α = 0.509, β = 0.33 × 10^8 cm, z_1 and z_2 are the charges of the reacting anions, and r is the hard-sphere collision distance, 1.12 nm). The result, plotted in Figure 4, gives a line (R^2 = 0.996) whose slope gives the charge product, z_1z_2, and whose y intercept gives k_{11} at μ = 0 (the self-exchange rate constant at zero ionic strength).

The slope of the plot in Figure 4 gives a charge product of z_1z_2 = 29 ± 2 (z_1 and z_2 are −6 and −5, the charges of 1$_{red}$ and 1$_{ox}$). Close agreement with the theoretical value (z_1z_2 = 30) shows compliance with the extended Debye−Hückel

(64) Swift, T. J. In *NMR of Paramagnetic Molecules: Principles and Applications*; La Mar, G. N., Horrocks, W. D., Jr., Holm, R. H., Eds.; Academic Press: New York, 1973; pp 53−84.
(65) Pethybridge, A. D.; Prue, J. E. In *Inorganic Reaction Mechanisms Part II*; Edwards, J. O., Ed.; John Wiley & Sons: New York, 1972; Vol. 17, pp 327−390.
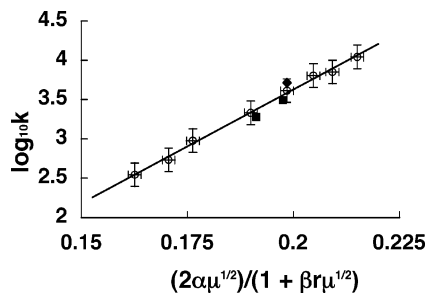
Figure 4. Plot of log k for electron self-exchange between $\mathbf{1}_{ox}$ and $\mathbf{1}_{red}$ as a function of ionic strength, μ. From the extended Debye−Hückel equation, $\log k = \log k_0 + 2z_1z_2\alpha\mu^{1/2}/(1 + \beta r\mu^{1/2})$ ($\alpha = 0.509$, $\beta = 0.33 \times 10^8$ cm, and r is the hard-sphere collision distance, 1.12 nm); the slope ($R^2 = 0.996$) gives the charge product, z_1z_2, and the y intercept (at $\mu = 0$) gives k_{11}. Rate constants were obtained using total heteropolyanion concentrations, [POM]$_{total}$, of 4.6 mM at pH 7.2 (O) and pH 2.15 (♦); two rate constants (■) were obtained at pH 7.2, but with [POM]$_{total}$ = 9.2 mM. Uncertainties (shown as error bars here)in k_{11} and in z_1z_2 (reported in the text) are 95% confidence intervals.

equation,[66] a prerequisite to the defensible application of theoretical models, such as those of Marcus and Sutin, to outer-sphere electron-transfer reactions between charged donors and acceptors. The parameters used in the extended Debye−Hückel equation ($\alpha = 0.509$ and $\beta = 0.33 \times 10^8$ cm; see caption of Figure 4) are standard values for ions in water at 25 °C. The charge product of 29 ± 2, thus, indicates that (1) $\mathbf{1}_{red}$ and $\mathbf{1}_{ox}$ behave in aqueous NaCl as charged, −6 and −5, spheres, each with of radius 5.6 Å,[27] (2) ion pairing with Na$^+$ is negligible at NaCl concentrations as large as 1 M (cf., entry 12 in Table 6), and (3) cation (Na$^+$) catalysis[67] of the electron exchange between the two ions is not kinetically significant. (See the Supporting Information for data on electron self-exchange reactions between α-AlW$_{12}$O$_{40}$$^{7-}$ and α-AlW$_{12}$O$_{40}$$^{6-}$, β-AlW$_{12}O_{40}$$^{6-}$ and

(66) Solutions of *mixed* electrolytes, such as those almost always encountered in kinetic studies in water, do not *rigorously* satisfy the thermodynamic criteria for which the extended Debye−Hückel equation was derived (see Pethybridge, A. D.; Prue, J. E. Kinetic salt effects and the specific influence of ions on rate constants. In *Progress in Inorganic Chemistry*; Lippard, S. J., Ed.; Vol. 17; *Inorganic Reaction Mechanisms Part II*, Edwards, J. O., Ed.; John Wiley & Sons: New York, 1972; pp 327−390). At the same time, other models, such as the full Guggenheim equation, while rigorously correct thermodynamically, were not derived for highly charged POM cluster anions and, furthermore, are strictly applicable only to solutions whose ionic strengths do not exceed 0.1 M. Attempts to model our data using the Debye−Hückel or Guggenheim equations gave incorrect theoretical charge products (i.e., theoretical values were off by more than 50%). Notably, the Guggenheim equation eliminates explicit use of r, the distance of closest approach of the reacting ions, and, instead, introduces interaction coefficients, B, as empirical corrections to the Debye−Hückel equation. The extended Debye−Hückel equation (eq 4 on page 331 in Perthybridge and Prue), on the other hand, *explicitly includes the distance of closest approach, r, of the colliding ions*. In Figure 4, we fixed r at twice the crystallographic radius of a Keggin anion and obtained a slope that gave a theoretical charge product effectively identical to that present in our exchanging system. We, therefore, suspect that the explicit inclusion of the distance of closest approach may be critically important. Additional compelling arguments for using the extended Debye−Hückel equation in Figure 4 were that (1) Kozik and Baker applied this equation in a study of outer-sphere electron transfer between Keggin anions in water and not only obtained expected charge products but also found remarkably close agreement between experimental rate constants (by extrapolation of the extended Debye−Hückel-equation plot to zero ionic strength) and those predicted by Sutin's semiempirical model and (2) use of the extended Debye−Hückel equation in our work makes it possible to compare our results with those of Kozik and Baker.
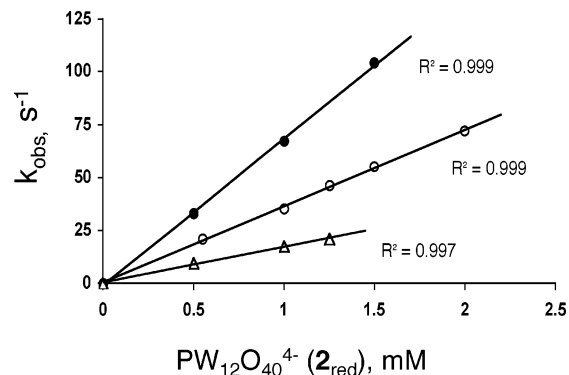(67) Metelski, P. D.; Swaddle, T. W. *Inorg. Chem.* **1999**, *38*, 301−307.

Figure 5. Rate constants, k_{obs}, for the oxidation α-AlW$_{12}$O$_{40}$$^{6-}$ ($\mathbf{1}_{red}$; limiting reagent) by α-PW$_{12}$O$_{40}$$^{4-}$ ($\mathbf{2}_{red}$; present at large molar excess) at three initial ionic strength values (μ, adjusted by addition of NaCl), 65 (▲), 97 (O), and 140 (●) mM, in 50 mM phosphate buffer (pH 2.15) at 25 °C. The points at the origin are for [$\mathbf{2}_{red}$] = 0 mM, at which no reaction occurs ($k_{obs} = 0$ s^{-1}).

β-AlW$_{12}$O$_{40}$$^{5-}$, and β-AlW$_{12}O_{40}$$^{7-}$ and β-AlW$_{12}$O$_{40}$$^{6-}$. In all cases, Debye−Hückel plots similar to that in Figure 4 give charge products within the experimental uncertainty of theoretical values.)

The rate of self-exchange varied with μ, but not with pH. While most of the data in Figure 4 were obtained at pH 7.2 (phosphate buffer), the rate constant at pH 2.15 (sulfate buffer; solid diamond in Figure 4) fell within experimental uncertainty of the line described by the data obtained at pH 7.2. In an additional control experiment, pertinent to the variation of [$\mathbf{1}_{red}$] in kinetic studies of reductions in water, two rate constants (solid squares in Figure 4) were obtained after doubling [POM$_{total}$] values to 9.2 mM. Finally, extrapolation of the plot in Figure 4 to zero ionic strength ($\mu = 0$) gave $k_{11} = (6.5 \pm 1.5) \times 10^{-3}$ M^{-1} s^{-1}.[68]

Independent Verification of k_{11}. The self-exchange rate constant, k_{11}, for the $\mathbf{1}_{red}/\mathbf{1}_{ox}$ pair was confirmed through an independent line of experimental evidence. This involved measuring the rate of electron transfer from $\mathbf{1}_{red}$ to α-PW$_{12}$O$_{40}$$^{4-}$ ($\mathbf{2}_{red}$; one-electron reduced) to give α-PW$_{12}$O$_{40}$$^{5-}$ (the two-electron reduced ion). Initially, and logically, the reaction between $\mathbf{1}_{red}$ and the fully oxidized ion, α-PW$_{12}$O$_{40}$$^{3-}$, $\mathbf{2}_{ox}$, was studied. However, this reaction exhibited polymodal kinetics, a complication likely due to the intermediate (and transient) formation of $\mathbf{2}_{red}$. This complication was avoided by reacting $\mathbf{1}_{red}$ with $\mathbf{2}_{red}$, rather than with $\mathbf{2}_{ox}$. [Experimentally measured rate constants (determined by ^{31}P NMR) have been reported for both electron self-exchange reactions: α-PW$_{12}$O$_{40}$$^{4-}$ + α-PW$_{12}$O$_{40}$$^{3-}$ and α-PW$_{12}$O$_{40}$$^{5-}$ + α-PW$_{12}$O$_{40}$$^{4-}$.[25]]

Solutions of $\mathbf{1}_{red}$ and $\mathbf{2}_{red}$ were mixed in a stopped-flow apparatus coupled to a UV−vis spectrophotometer. The increase in absorbance was exponential, and pseudo-first-order rate constants, k_{obs}, were determined from each entire absorbance-versus-time curve. Plots of these rate constants as a function of initial $\mathbf{2}_{red}$ concentration, at three ionic-strength values, gave straight lines (three lines in Figure 5). The slopes of these lines are the bimolecular rate constants

(68) Experimental uncertainties were calculated using "Data Analysis ToolPak: Regression" from Microsoft Excel.
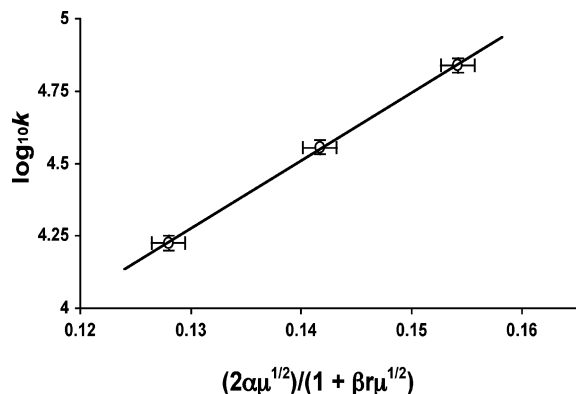
Figure 6. Extended Debye–Hückel equation plot of rate constants for electron transfer from $\mathbf{1}_{red}$ to $\mathbf{2}_{red}$; $R^2 = 0.9997$, the slope gives a charge product, z_1z_2, of 23 ± 1, and extrapolation to zero ionic strength ($\mu = 0$) gives $k_0 = 17 \pm 2$ M^{-1} s^{-1}. Changes in ionic strength during the reaction—because of changes in the charges of the reacting species—were small relative to the total ionic strength and relative to the statistical uncertainty involved in extrapolation to $\mu = 0$.

for the reaction at each of the three ionic-strength values studied. The range of experimentally useful ionic strength values was rather limited. At large μ values, the reaction occurred too rapidly (accurate rate data could not be obtained). On the other hand, μ values could not be decreased indiscriminately because the POMs themselves contributed significantly to μ and also because minimum electrolyte concentrations were needed to carry out the bulk electrolysis reactions used to prepare $\mathbf{1}_{red}$ and $\mathbf{2}_{red}$.

Bimolecular rate constants, obtained at three experimentally accessible ionic-strength values, were plotted as a function of ionic strength using the extended Debye–Hückel equation (Figure 6). The slope gave a charge product (z_1z_2; product of the charges of $\mathbf{1}_{red}$ and $\mathbf{2}_{red}$) of 23 ± 1, within experimental uncertainty of the theoretical values of 24. Extrapolation to zero ionic strength gave $k_0 = 17 \pm 2$ M^{-1} s^{-1}.

The rate constant for self-exchange between $\mathbf{1}_{red}$ and $\mathbf{1}_{ox}$, obtained by ^{27}Al NMR [$(6.5 \pm 1.5) \times 10^{-3}$ M^{-1} s^{-1}], was then evaluated by using it in the Marcus cross-relation to estimate $k_{0(calc)}$ for electron transfer from $\mathbf{1}_{red}$ to $\mathbf{2}_{red}$ at zero ionic strength. Also used in this calculation were the published[25] rate constant for self-exchange between $\mathbf{2}_{red}$ and α-PW$_{12}$O$_{40}$$^{5-}$ [$(1.6 \pm 0.3) \times 10^2$ M^{-1} s^{-1}] and the reduction potentials, -130 ± 5 and -10 ± 5 mV, respectively, for the self-exchanging couples, $\mathbf{1}_{red}/\mathbf{1}_{ox}$ and $\mathbf{2}_{red}/\alpha$-PW$_{12}$O$_{40}$$^{5-}$. All work-term corrections,[69] though small, were included. The Marcus cross-relation gave $k_{0(calc)} = 13 \pm 6$ M^{-1} s^{-1}. This value, within experimental uncertainty of that obtained by stopped-flow measurements (17 ± 2 M^{-1} s^{-1}; from Figure 6), provides independent verification of the rate constant [$k_{11} = (6.5 \pm 1.5) \times 10^{-3}$ M^{-1} s^{-1}], determined by ^{27}Al NMR for self-exchange between $\mathbf{1}_{red}$ and $\mathbf{1}_{ox}$.[70]

Discussion

Detailed Evaluation of k_{11}. To date, the most reliable rate-constant values for self-exchange between Keggin anions

were published in 1990, by Kozik and Baker, for reactions between α-PW$_{12}$O$_{40}$$^{3-}$ ($\mathbf{2}_{ox}$), α-PW$_{12}$O$_{40}$$^{4-}$ ($\mathbf{2}_{red}$; one-electron reduced), and α-PW$_{12}$O$_{40}$$^{5-}$ (two-electron reduced).[25] Rates of self-exchange as a function of ionic strength were measured by ^{31}P NMR spectroscopy (rapid exchange limit).

In that study, Kozik and Baker successfully used the extended Debye–Hückel equation to evaluate six rate constants, k, obtained at μ values that ranged from 0.26 to 0.616 M. All six k values lay on a straight line (correlation coefficient = 0.998), whose slope gave a charge product, z_1z_2, of 14.1, relatively close to the theoretical z_1z_2 value of 12. The authors commented that the extended Debye–Hückel equation "adequately accounts for the ionic strength dependence of the rate constant even at rather unexpectedly high ionic strengths (>0.500 M), even though the equation was originally derived only for ionic concentrations smaller than 0.01 M." They suggest this may be a consequence of the "fact that heteropoly anions, owing to the very pronounced inward polarization of their exterior oxygen atoms, have extremely low solvation energies and very low van der Waals attractions for one another." This is consistent with our observation that very little ion pairing between $\mathbf{1}$ and Na$^+$ or H$^+$ occurs over wide ranges of concentrations of these cations. An additional relevant factor is that POM-anion charges, distributed over many atoms, are highly diffuse, more so than for anions typically viewed as "noncoordinating." For example, while the single charge of perchlorate (ClO$_4$$^-$) is distributed over five atoms (a ratio of 1:5, or 0.2), the -6 charge of $\mathbf{1}_{red}$ is distributed over 53 atoms (a ratio of 0.11). The diffuse nature of the POM charge is even more pronounced when compared with ions in simple salts, such as NaCl, for which the extended Debye–Hückel equation was originally derived.[71] These observations are supported by the results of diffusion-rate[72,73] and density[74] measurements, which, on the basis of the application of the Stokes–Einstein equation,[26,75] argue that the effective hydrodynamic radii of 3-, 4-, 5-, and 6- Keggin anions are *equal to* their

(69) Marcus, R. A.; Sutin, N. *Biochim. Biophys. Acta* **1985**, *811*, 265–322.

(70) Note added in proof: In a work to be reported separately (see Proceedings of the 9th International Symposium on the Activation of Dioxygen and Catalytic Homogeneous Oxidation; Cologne, Germany, July 25–29, 2005, page 44), the Marcus cross relation, in conjunction with the experimentally determined rate constant for self-exchange between O$_2$ and O$_2$$^-$ (superoxide radical anion) of $k_{11} = 450$ M^{-1} s^{-1} (Lind, J.; Chen, X.; Merényi, G.; Lund, J.; Jonsson, B. O. *J. Am. Chem. Soc.* **1989**, *111*, 7654–7655), and the self-exchange rate constant, k_{11}, for the $\mathbf{1}_{red}/\mathbf{1}_{ox}$ pair reported here [$(6.5 \pm 1.5) \times 10^{-3}$ M^{-1} s^{-1}] gives a theoretical rate constant for electron transfer from $\mathbf{1}_{red}$ to O$_2$ of 16 ± 9 M^{-1} s^{-1}. The experimental rate constant for this reaction at pH 7 is 24 ± 2 M^{-1} s^{-1}. This close agreement—the two values are statistically identical—provides additional, and compelling, experimental confirmation regarding the accuracy of the rate constant, k_{11}, for the $\mathbf{1}_{red}/\mathbf{1}_{ox}$ pair, reported here.

(71) Alternatively, a comparison can be made on the basis of anion-charge densities (anion charge, q/radius). From this perspective, ClO$_4$$^-$ has a thermochemical radius of 2.36 Å and a charge density ($|q/r|$) of 0.42/Å, while $\mathbf{2}_{red}$ (a -4 anion) and $\mathbf{1}_{red}$ (a -6 anion) both have crystallographic radii of 5.6 Å and charge densities, respectively, of 0.71/Å and 1.07/Å.

(72) Baker, M. C.; Lyons, P. A.; Singer, S. J. *J. Am. Chem. Soc.* **1955**, *77*, 2011–2012.

(73) Grigoriev, V. A.; Hill, C. L.; Weinstock, I. A. *J. Am. Chem. Soc.* **2000**, *122*, 3544–3545.

(74) Kurucsev, T.; Sargeson, A. M.; West, B. O. *J. Phys. Chem.* **1957**, *61* (1), 1567–1569.

(75) Edward, J. T. *J. Chem. Educ.* **1970**, *47*, 261–270.

crystallographic radii. This means that, on average, the Keggin anions are each solvated by no greater than one water molecule. This result highlights the difference between solvated Keggin ions and aqueous solutions of familiar alkali-metal cations such as Li^+ and Na^+, whose hydrodynamic radii of 3.40 and 2.76 Å suggest a strong association of each ion, respectively, with 25 and 17 water molecules.[76]

For self-exchange between $\mathbf{2}_{ox}$ and $\mathbf{2}_{red}$, Kozik and Baker reported a rate constant (at $\mu = 0$) of $(1.1 \pm 0.2) \times 10^5$ M^{-1} s^{-1}.[77] This value is more than 7 orders of magnitude larger than that reported here for self-exchange between $\mathbf{1}_{red}$ and $\mathbf{1}_{ox}$. The difference between these two rate constants is due to differences between associated charge products—$z_1 z_2$ (12 and 30, respectively, for the P- and Al-containing ions)— and, to a much lesser extent, to differences between total reorganization energies, λ_{total}. The contribution of each of these parameters to k_{11} for self-exchange between $\mathbf{1}_{red}$ and $\mathbf{1}_{ox}$ was calculated by applying the semiclassical model[42] that Kozik and Baker used to a estimate self-exchange rate-constant for the P(V)-containing anions.

Kozik and Baker used data from a normal-coordinate analysis of the IR spectrum of a related cluster anion (hexatungstate; $W_6O_{19}^{2-}$)[78] to estimate the inner-sphere reorganization energy for self-exchange between $\mathbf{2}_{ox}$ and $\mathbf{2}_{red}$. The value they calculated, $\lambda_{in} = 6.1$ kcal mol^{-1}, when used in the semiclassical model,[42] gave a theoretical self-exchange value of 3.6×10^5 M^{-1} s^{-1}. Using their *experimental* value [$k_{11} = (1.1 \pm 0.2) \times 10^5$ M^{-1} s^{-1}], the semiclassical model gives a slightly larger value of $\lambda_{in} = 8.8$ kcal mol^{-1}. By comparison, an analysis of k_{11} for the reaction between $\mathbf{1}_{red}$ and $\mathbf{1}_{ox}$ [$(6.5 \pm 1.5) \times 10^{-3}$ M^{-1} s^{-1}], using the semiclassical model (and parameters identical or analogous, as appropriate, to those used by Kozik and Baker),[25] gives an inner-sphere reorganization energy, λ_{in}, of 16.1 kcal mol^{-1}. Values of λ_{out}, which change little between the two systems, are 16.4 and 16.5 kcal mol^{-1} for the $\mathbf{2}_{red}/\mathbf{2}_{ox}$ and $\mathbf{1}_{red}/\mathbf{1}_{ox}$ pairs, respectively, and give total reorganization energies, λ_{total}, of 25.2 kcal mol^{-1} for $\mathbf{2}_{red}/\mathbf{2}_{ox}$ and 32.6 kcal mol^{-1} for $\mathbf{1}_{red}/\mathbf{1}_{ox}$.

The difference in λ_{in} values may be due to differences between the bond lengths and bond angles associated with the 12 $X-\mu_4-O-W$ linkages within the $X = P(V)$ and $X = Al(III)$ Keggin ions,[27] and the effect of these differences on force constants (related to IR stretching frequencies), that sum to λ_{in}.[25] Notably, when $X = Al(III)$, the μ_4-O-W bonds [four μ_4-O atoms are bonded to Al(III) and 12 μ_4-O-W bonds are trans to the terminal W=O bonds in the 12 C_{4v}-symmetry WO_6 polyhedra] are shorter and possess larger force constants than when $X = P(V)$. During electron exchange, this could conceivably (depending upon the nature of the LUMO) be multiplied over all 12 of these linkages. The attribution of variation in λ_{in} values to structural differences between $\mathbf{1}_{ox}$ and $\mathbf{2}_{ox}$ is consistent with the
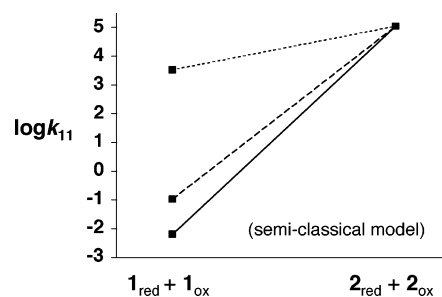

Figure 7. Zero-ionic-strength self-exchange rate constants for electron transfer between α-$AlW_{12}O_{40}^{6-}$ and α-$AlW_{12}O_{40}^{5-}$ ($\mathbf{1}_{red}$ and $\mathbf{1}_{ox}$) and between α-$PW_{12}O_{40}^{4-}$ and α-$PW_{12}O_{40}^{3-}$ ($\mathbf{2}_{red}$ and $\mathbf{2}_{ox}$). The rate constant for self-exchange between $\mathbf{2}_{red}$ and $\mathbf{2}_{ox}$ is at the upper right ($k_{11} = 1.1 \times 10^5$ M^{-1} s^{-1}; log $k_{11} = 5.04$), and that for self-exchange between $\mathbf{1}_{red}$ and $\mathbf{1}_{ox}$ is at the lower left ($k_{11} = 6.5 \times 10^{-3}$ M^{-1} s^{-1}; log $k_{11} = -2.19$). See the text for descriptions of the three lines shown.

documented effects of the heteroatom, X, on key properties of Keggin ions. For example, X-ray crystallographic data[27,29] and theoretical calculations[34] both show that the relative energies of α- and β-Keggin isomers are strongly influenced by the nature of the heteroatom and its influence on cluster-anion structure [a clear trend is observed as X is varied from P(V) to Si(IV) to Al(III)].

The remaining difference between the self-exchange rate constants is attributed to the difference in charge products, $z_1 z_2$. The effects of both λ_{total} values and charge products, calculated using the semiclassical model, are shown in Figure 7.[79] The dotted line (top) shows the decrease in k_{11} associated with an increase in λ_{total} of 25.2 kcal mol^{-1} for $\mathbf{2}$ to 32.6 kcal mol^{-1} for $\mathbf{1}$; the dashed line (middle) shows the decrease in k_{11} associated with an increase in the charge product, $z_1 z_2$, from 12 for self-exchange between $\mathbf{2}_{red}$ and $\mathbf{2}_{ox}$ to 30 for self-exchange between $\mathbf{1}_{red}$ and $\mathbf{1}_{ox}$. The decrease in rate as $z_1 z_2$ increases from 12 to 30 is due to the associated increase in electrostatic repulsion between the colliding anions. More specifically, the Coulombic work terms (energies) associated with the formation of the respective precursor complexes, $[(\mathbf{2}_{red})(\mathbf{2}_{ox})]^{12-}$ and $[(\mathbf{1}_{red})(\mathbf{1}_{ox})]^{30-}$, at zero ionic strength are 4.54 kcal mol^{-1} for $z_1 z_2 = 12$ and 11.2 kcal mol^{-1} for $z_1 z_2 = 30$.

In summary, the data in Figure 5 show that the rate constant for self-exchange between $\mathbf{1}_{red}$ and $\mathbf{1}_{ox}$ is fully accounted for by the semiclassical model. Moreover, this comparison between $\mathbf{2}_{red}/\mathbf{2}_{ox}$ and $\mathbf{1}_{red}/\mathbf{1}_{ox}$ pairs provides a rare opportunity for observing the effects of very large charge products, $z_1 z_2$, on electron exchange between nearly iso-structural ions.

Conclusions

Use of $\mathbf{1}_{red}$ as a Mechanistic Probe. The above data recommend $\mathbf{1}_{red}$ as a well-behaved probe for investigating

(76) Cotton, F. A.; Wilkinson, G. *Advanced Inorganic Chemistry*, 4th ed.; Wiley: New York, 1980.

(77) For reaction between $\mathbf{2}_{red}$ and α-$PW_{12}O_{40}^{5-}$ (two-electron reduced), Kozik and Baker (ref 25) reported a rate constant (at $\mu = 0$) of $(1.6 \pm 0.3) \times 10^2$ M^{-1} s^{-1}.

(78) Rocchiccioli-Deltcheff, C.; Fournier, M.; Franck, R.; Thouvenot, R. *J. Mol. Struct.* **1984**, *114*, 49−56.

(79) To our knowledge, a reliable rate constant for self-exchange between $SiW_{12}O_{40}^{5-}$ (one-electron reduced) and $SiW_{12}O_{40}^{4-}$ has not been reported. However, estimations based on the following series of reactions of isostructural Keggin anions, $\mathbf{1}_{red} + O_2$, $SiW_{12}O_{40}^{5-} + O_2$, and $\mathbf{2}_{red} + O_2$ (to be reported separately; see ref 70), give a self-exchange rate constant whose value lies between those shown in Figure 7 and which is consistent with $z_1 z_2 = 20$ and a total reorganization energy, λ_{total}, between 25 and 32 kcal mol^{-1}.

outer-sphere electron transfer to chemically, biologically, or technologically important molecules or nanostructures in water. First, we here provide accurate and reliable thermodynamic and kinetic values, respectively, for the reduction potential, $E_{1/2}$, and the zero-ionic-strength ($\mu = 0$) rate constant, k_{11}, for electron self-exchange between $\mathbf{1}_{red}$ and fully oxidized $\mathbf{1}_{ox}$. These values allow $\mathbf{1}_{red}$, an outer-sphere electron donor, to be used as a well-behaved and kinetically well-defined mechanistic probe.[37] Equally important, $\mathbf{1}_{red}$ is stable to isomerization (kinetically, at temperatures of 0 to at least 60 °C), disproportionation, and acid condensation or hydrolysis, at pH values of 0−7.5. Critically, over most of this pH range (from pH 1.8 to 7.5), $\mathbf{1}_{red}$ is entirely free of close association with H_3O^+ and can, therefore, be used in variable pH studies designed to investigate "coupling" between the protonation and outer-sphere reduction of electron acceptors.[41] In addition, the data in Table 6 and Figure 4 show that $\mathbf{1}_{red}$ is effectively free of ion pairing with Na^+ at NaCl concentrations as large as 1.0 M and can, therefore, be used in studies that require that aqueous sodium salts be present and in variable ionic-strength studies designed to evaluate the kinetic consequences of electron-acceptor charge. Ongoing and future mechanistic studies using $\mathbf{1}_{red}$ include electron transfer to small molecules such as O_2,[80] H_2, or NO; to biomimetic metallo-organic complexes, and to redox-active enzymes and include the use of $\mathbf{1}_{red}$ to provide fundamental information regarding relationships between cation motion (Na^+ and others) and charge transfer, in controlled reductions of metal, metal oxide, or semiconductor quantum dots.[81]

Electron Exchange between Uniformly Charged Nanospheres. As demonstrated by the data in Figure 4, the extended Debye−Hückel equation appears to describe the effect of ionic strength—at relatively large electrolyte concentrations—on collision rates between highly charged Keggin heteropolytungstate cluster anions. While these anions possess relatively high charges, their electron densities are diffuse and uniformly distributed over the entire nanom-

eter-sized (1.12 nm diameter) and highly symmetric (formally T_d, but effectively spherical) structure. At the same time, the extended Debye−Hückel equation, and similar models, were originally derived for collisions between ions of much smaller charge (typically 1:1 or 1:2 electrolytes) and at very low ionic strengths. Given this, the present work, combined with other studies that document electron exchange between POM cluster anions, may argue for the development of a new theoretical model, specifically derived to describe collision rates between uniformly charged nanospheres or nanoparticles, for which POMs provide a working model.

Supporting Information Available: Methods for calibration of the Ag/AgCl (3 M NaCl) BAS reference electrode and for titrimetric determination of α-AlW$_{12}$O$_{40}^{6-}$ ($\mathbf{1}_{red}$) concentrations; a cyclic voltammogram of α-AlW$_{12}$O$_{40}^{5-}$ (first and second one-electron reductions, Figure S1); cyclic voltammetric and ^{27}Al NMR data for α- and β-Na$_5$AlW$_{12}$O$_{40}$ before and after cycles of electrochemical reduction and electrochemical or chemical reoxidation (Table S1); extinction coefficients, ϵ, as a function of λ (in nm), for α-AlW$_{12}$O$_{40}$,[6−] α-PW$_{12}$O$_{40}$,[4−] and α-PW$_{12}$O$_{40}^{5-}$ (Figure S2); experimental details and crystal data and structure refinement parameters for α-Cs$_6$Na[AlW$_{12}$O$_{40}$]·14.5H$_2$O (Table S2); positional and thermal parameters and bond lengths and angles in CIF format; Extended Debye−Hückel plots; and tabulated data (charge products and zero-ionic strength rate constants for electron self-exchange reactions between α-AlW$_{12}$O$_{40}^{7-}$ and α-AlW$_{12}$O$_{40}^{6-}$, β-AlW$_{12}$O$_{40}^{6-}$ and β-AlW$_{12}$O$_{40}^{5-}$, and β-AlW$_{12}$O$_{40}^{7-}$ and β-AlW$_{12}$O$_{40}^{6-}$, Figures S3 and S4 and Table S3). This material is available free of charge via the Internet at http:// pubs.acs.org.

IC050860M

---

(80) In a work to be reported separately (see refs 70 and 79), an isostructural series of one-electron-reduced α-Keggin heteropolytungstate cluster anions (POM$_{red}$: α-X^{n+}W$_{12}$O$_{40}^{(n-9)-}$, where X^{n+} = Al^{III}, Si^{IV}, P^V), whose charges vary with X^{n+} from −6 to −5 to −4, and whose one-electron (POM$_{ox}$/POM$_{red}$) reduction potentials, $E_{1/2}$, vary, respectively, from −0.130 to +0.055 to +0.255 V (NHE), are used to define the roles of both H$^+$ (variable-pH studies using $\mathbf{1}_{red}$) and POM charge (use of all three donor anions at pH 2) in outer-sphere electron transfer to O$_2$ in water: POM$_{red}$ + O$_2$ + H$^+$ → POM$_{ox}$ + HO$_2$·

(81) Such studies address the need for fundamental information concerning charge transfer at the nanoscale and the "coupling" of ion motion to interfacial charge transfer within nanoscale electronic devices. For an overview of this general problem, see: Adams, D. M.; Brus, L.; Chidsey, C. E. D.; Creager, S.; Creutz, C.; Kagan, C. R.; Kamat, P. V.; Lieberman, M.; Lindsay, S.; Marcus, R. A.; Metzger, R. M.; Michel-Beyerle, M. E.; Miller, J. R.; Newton, M. D.; Rolison, D. R.; Sankey, O.; Schanze, K. S.; Yardley, J.; Zhu, X. *J. Phys. Chem. B* **2003**, *107*, 6668−6697.